

Ruthenium(II) Complexes Containing Anti-Inflammatory Drugs as Ligands: Synthesis, Characterization and *in vitro* Cytotoxicity Activities on Cancer Cell Lines

Junai C. S. Lopes,^{a,b} Jaqueline L. Damasceno,^c Pollyanna F. Oliveira,^c
Adriana P. M. Guedes,^d Denise C. Tavares,^c Victor M. Defflon,^e Norberto P. Lopes,^f
Marcos Pivatto,^b Alzir A. Batista,^d Pedro I. S. Maia^g and Gustavo Von Poelhsitz^{*,b}

^aInstituto Federal Norte de Minas Gerais, Campus Pirapora, CP 54, 39270-000 Pirapora-MG, Brazil

^bInstituto de Química, Universidade Federal de Uberlândia, CP 593, 38400-902 Uberlândia-MG, Brazil

^cUniversidade de Franca, 14404-600 Franca-SP, Brazil

^dDepartamento de Química, Universidade Federal de São Carlos, CP 676, 13561-901 São Carlos-SP, Brazil

^eInstituto de Química de São Carlos, Universidade de São Paulo, CP 780, 13566-590 São Carlos-SP, Brazil

^fNúcleo de Pesquisa em Produtos Naturais e Sintéticos (NPPNS), Faculdade de Ciências Farmacêuticas de Ribeirão Preto, Universidade de São Paulo, 14040-903 Ribeirão Preto-SP, Brazil

^gInstituto de Ciências Naturais, Exatas e Educação, Universidade Federal do Triângulo Mineiro, 38064-200 Uberaba-MG, Brazil

The synthesis, characterization and cytotoxic activity of *cis*-[Ru(dicl)(dppm)₂]PF₆ and *cis*-[Ru(ibu)(dppm)₂]PF₆, (dppm = 1,1-bis(diphenylphosphine)methane; dicl = diclofenac anion and ibu = ibuprofen anion), are described in this work. Complexes were characterized by elemental analysis, Fourier transform infrared spectroscopy (FTIR), UV-Vis, ³¹P{¹H} nuclear magnetic resonance (NMR) and high-resolution mass spectrometry (HRESIMS). X-ray structure of *cis*-[Ru(ibu)(dppm)₂]PF₆ is also described. Preliminary calf thymus DNA (ct-DNA) binding studies were carried out by UV-Vis and viscosity experiments, with results suggesting the existence of electrostatic interactions between ruthenium complexes and ct-DNA. Cytotoxicity assays were carried out on a panel of human cancer cell lines and a human normal cell line. Complexes displayed a high to moderate cytotoxicity with IC₅₀ ranging from 5 to 47 μmol L⁻¹. *cis*-[Ru(ibu)(dppm)₂]PF₆ was found to be the most active, with IC₅₀ values lower than cisplatin. The degree of cytotoxicity was maintained for the normal cell line, although *cis*-[Ru(ibu)(dppm)₂]PF₆ exhibited a similar selectivity to that of cisplatin but with a higher activity for at least two tumor cell lines which evidences a promising anticancer candidate and selects this complex for further experiments.

Keywords: ruthenium(II) complexes, cytotoxic activity, sodium diclofenac, sodium ibuprofen, dppm

Introduction

The disseminated use of cisplatin and other platinum based metallodrugs as chemotherapeutic agents against ovarian, bladder and testicular cancers, among others, is still a key aspect for the development of the medicinal inorganic chemistry.¹⁻⁶ In the search for coordination compounds which are active against tumors and less toxic than cisplatin, ruthenium compounds emerge as the most promising

candidates.⁵⁻⁷ Their interesting biological features include the mechanism of action, toxicity and biodistribution which differ from those of classical platinum compounds and might therefore be active against cisplatin resistant human cancers.^{5,7-11} In the last years, three ruthenium complexes (Figure 1) have entered in clinical trials: [InH][*trans*-RuCl₄(In)₂] (KP1019) and Na[*trans*-RuCl₄(In)₂] (In = indazole) (NKP1339) that displayed high activity in primary tumor models and [ImH][*trans*-RuCl₄(DMSO)(Im)] (NAMI-A) which showed effect against solid tumor metastases.^{9,12-15}

*e-mail: gustavo@iqufu.ufu.br



In this work the synthesis and characterization of two new ruthenium(II) derivatives with formula [Ru(dicl)(dppm)₂]PF₆ (**1**) and [Ru(ibu)(dppm)₂]PF₆ (**2**) are reported. Furthermore, preliminary binding properties to calf thymus DNA (ct-DNA) and *in vitro* tests of cytotoxic activities against a panel of human cell lines are presented and discussed.

Infrared spectra (IR) were obtained on a PerkinElmer Spectrum Two spectrophotometer equipped with an attenuated total reflectance (ATR) sample holder and ZnSe crystal. The spectra were recorded in the range of 4000-600 cm^{-1} with a 4 cm^{-1} resolution. UV-Vis spectroscopy was performed on a Shimadzu UV2501 PC spectrophotometer using cuvettes with a 1 cm path length and methanol as solvent. $^{31}\text{P}\{^1\text{H}\}$ nuclear magnetic resonance (NMR) was performed on a Bruker DRX 400 MHz spectrometer with a BBO 5 mm probe at 298 K. The NMR spectra were recorded in CH_2Cl_2 using a capillary of D_2O to get the lock and with H_3PO_4 (85%) as external reference. Conductance data, obtained at 298 K on 1×10^{-3} mol L^{-1} methanol solutions of the complexes, were measured with a Tecnonon MCA 150 conductometer. Elemental analyses were performed on a Perkin Elmer 2400 Series II CHNS/O microanalyser. High-resolution mass spectra (HRESIMS) with electrospray ionization were measured on an ultratOF (Bruker Daltonics) spectrometer, operating in the positive mode. Methanol was

used as solvent system and the samples were infused into the ESI source at a flow rate of 5 $\mu\text{L min}^{-1}$. The calculated values for the charged complex ions were made by using ChemBioDraw Ultra 14.0.

Synthesis

The precursor *cis*-[RuCl₂(dppm)₂] (0.103 mmol; 100 mg) was solubilized in 50 mL of methanol, followed by the direct addition of sodium diclofenac (0.120 mmol; 37.2 mg) or sodium ibuprofen (0.120 mmol; 26.6 mg), respectively, for synthesis of the complexes **1** and **2**. The resulting solution was stirred at room temperature for a 6 h period. The final solution was concentrated to ca. 5 mL and an aqueous solution of NH₄PF₆ (0.150 mmol; 24.4 mg) was added for the precipitation of a yellow solid. The solid was filtered off and washed with water (3 \times 5 mL) and diethyl ether (3 \times 5 mL) and dried under reduced pressure.

[Ru(dicl)(dppm)₂]PF₆ (**1**)

Yield: 60.0 mg (85.5%); anal. calcd. for C₆₄H₅₄Cl₂F₆NO₂P₅Ru: exptl. (calcd.) C 58.68 (58.57), H 4.16 (4.26), N 1.07 (1.18); λ / nm (ϵ / L mol⁻¹ cm⁻¹) 229 (4.60 \times 10⁴), 257 (2.90 \times 10⁴), 288 (7.60 \times 10³), 338 (2.10 \times 10³); IR (ATR) ν / cm⁻¹ 3344, 3058, 3026, 2925, 2854, 1565, 1522, 1484, 1468, 1452, 1436, 1392, 1366, 1314, 1100, 1000, 949, 876, 837, 778, 731, 715, 694; ³¹P {¹H} NMR (162.0 MHz, CH₂Cl₂/D₂O) δ 8.2 (t, 2P, *J* 39.0 Hz), -12.8 (t, 2P, *J* 39.0 Hz); -144.7 (sep, 1P, *J* 711 MHz, PF₆⁻); HRESIMS *m/z* calcd. for C₆₄H₅₄Cl₂NO₂P₄Ru [M - PF₆]⁺: 1164.1520; found: 1164.1520.

[Ru(ibu)(dppm)₂]PF₆ (**2**)

Yield: 57.0 mg (65.4%); anal. calcd. for C₆₃H₆₁F₆O₂P₅Ru: exptl. (calcd.) C 61.84 (62.02), H 5.47 (5.04); λ / nm (ϵ / L mol⁻¹ cm⁻¹) 227 (5.60 \times 10⁴), 257 (3.50 \times 10⁴), 340 (2.90 \times 10³); IR (ATR) ν / cm⁻¹ 3057, 2951, 2927, 2864, 1516, 1485, 1461, 1436, 1420, 1373, 1282, 1191, 1161, 1145, 1121, 1092, 1026, 1000, 905, 873, 834, 784, 763, 735, 727, 714, 694; ³¹P {¹H} NMR (162.0 MHz, CH₂Cl₂/D₂O) δ 8.3 (t, 2P, *J* 38.0 Hz), -12.3 (t, 2P, *J* 38 Hz); -144.7 (sep, 1P, *J* 711 Hz, PF₆⁻); HRESIMS *m/z* calcd. for C₆₃H₆₁O₂P₄Ru [M - PF₆]⁺: 1075.2660; found: 1075.2660.

X-ray crystallography

Yellow crystals of the complex **2** were grown by slow evaporation of a dichloromethane solution at room temperature. The data collection was performed using Mo-K α radiation (λ = 0.71073 Å) on a BRUKER APEX II Duo diffractometer. Standard procedures were applied

for data reduction and absorption correction. The structure was solved with SHELXS97 using direct methods²² and all non-hydrogen atoms were refined with anisotropic displacement parameters with SHELXL97.²³ The hydrogen atoms were calculated at idealized positions using the riding model option of SHELXL97.²³ Table 1 presents detailed information about the structural determination.

Table 1. Crystallographic data and structural refinement details for complex **2**

Empirical formula	C ₆₃ H ₆₁ F ₆ O ₂ P ₅ Ru
Molar mass / (g mol ⁻¹)	1220.04
Temperature / K	296
Crystal system	orthorhombic
Space group	Pna2(1)
Unit cell dimension	
a / Å	23.7204 (7)
b / Å	14.4607(5)
c / Å	17.3534(6)
V / Å ³	5952.5(3)
Z	4
Density (calcd.) / (g cm ⁻³)	1.361
Absorption coefficient / mm ⁻¹	0.459
F (000)	2512
Crystal size / mm ³	0.43 \times 0.42 \times 0.30
θ range data collection / degree	1.65 to 25.04
Index range	-24 \leq h \leq 28; -17 \leq k \leq 17; -15 \leq l \leq 20
Reflection collected	21774
Independent reflection	9009 [R(int) = 0.0190]
Completeness (to θ = 25.04°) / %	99.5
Absorption correction	semi-empirical from equivalents
Data / restraint / parameter	9009 / 16 / 766
Goodness-of-fit on F ²	1.041
Final R indices [I > 2sigma(I)]	R ₁ = 0.0243, wR ₂ = 0.0579
R indices (all data)	R ₁ = 0.0275, wR ₂ = 0.0600
Absolute structure parameter	-0.011(16)
Largest diff. peak and hole	0.308 and -0.189 e.Å ⁻³

DNA titration and viscosity experiments

A standard solution of ct-DNA was prepared in tris-HCl buffer (5 mol L⁻¹ tris-HCl, pH 7.2). The concentration of this ct-DNA solution was measured from its absorption intensity at 260 nm using the molar absorption coefficient value of 6600 mol⁻¹ L cm⁻¹. Solutions of ruthenium complexes **1** and **2** used in the experiments were prepared in Tris-HCl buffer containing 2% of dimethyl sulfoxide (DMSO). In the titration experiments, different concentrations of the ct-DNA were used while the ruthenium complex was at 20 $\mu\text{mol L}^{-1}$.

Viscosity experiments were carried out using an Ostwald viscometer maintained at a constant temperature of 25 °C in

a thermostatic bath. The viscosity of the ct-DNA solution was measured in the presence of increasing amounts of the complexes **1** and **2**. The flow times were measured with an automated timer. Each sample was measured three times, and an average flow time was calculated. The obtained data are presented as $(\eta/\eta_0)^{1/3}$ versus binding ratio ($[\text{Ru}]/[\text{DNA}]$), where η is the viscosity of ct-DNA in the presence of the complexes and η_0 is the viscosity of ct-DNA alone in buffer solution.²⁴⁻²⁶

Human cell lines and culture conditions

For the experiments, four different human cell lines from the 4th through 12th passages were used: HepG2 (hepatocellular carcinoma), MCF-7 (breast adenocarcinoma), MO59J (glioblastoma) and GM07492A (normal lung fibroblasts). The different cell lines were maintained as monolayers in plastic culture flasks (25 cm²) containing HAM-F10 plus Dulbecco's Modified Eagle Medium (DMEM), 1:1 (Sigma-Aldrich) or only DMEM, depending on the cell line, supplemented with 10% foetal bovine serum (Nutricell) and 2.38 mg mL⁻¹ Hepes (Sigma-Aldrich) at 37 °C in a humidified 5% CO₂ atmosphere. Antibiotics (0.01 mg mL⁻¹ streptomycin and 0.005 mg mL⁻¹ penicillin; Sigma-Aldrich) were added to the medium to prevent bacterial growth.

Cell viability assay related to human cell lines

Cytotoxic activity on the cell lines was assessed using the Colorimetric Assay *in vitro* Toxicology-XTT Kit (Roche Diagnostics) according to the manufacturer's instructions. For the experiments, 1×10^4 cells were seeded into microplates with 100 μL of culture medium (1:1 HAM F10 + DMEM or DMEM alone) supplemented with 10% fetal bovine serum containing concentrations of the ruthenium complexes ranging from 1.5625 to 1600 $\mu\text{g mL}^{-1}$. Negative (no treatment), solvent (0.02% DMSO) and positive (25% DMSO) controls were included. Positive controls comprising cisplatin (Sigma-Aldrich, $\geq 98\%$ purity) were included. After incubation at 36.5 °C for 24 h, the culture medium was removed and cells were washed with 100 μL of phosphate-buffered saline (PBS) to remove the treatments, after which they were exposed to 100 μL of HAM-F10 culture medium without phenol red. Then, 25 μL of XTT were added and the cells were incubated at 36.5 °C for 17 h. The absorbance of the samples was determined using a multi-plate reader (ELISA-Tecan-SW Magellan vs 5.03 STD 2P) at a wavelength of 450 nm and a reference length of 620 nm.

Statistical analysis related to human cell line assays

Cytotoxicity was assessed using the IC₅₀ response parameter (50% cell growth inhibition) calculated with the GraphPad Prism program, plotting cell survival against the respective concentrations of the treatments. One-way ANOVA was used for the comparison of means ($p < 0.05$). The selectivity index was calculated by dividing the IC₅₀ value of the isolated compounds on GM07492-A cells by the IC₅₀ value determined for human cancer cells.

Results and Discussion

Synthesis

The reaction of sodium salts of diclofenac and ibuprofen with the ruthenium(II) diphosphine precursor complex *cis*-[RuCl₂(dppm)₂] resulted in the products **1** and **2** by chlorido exchange under mild conditions as showed in Scheme 1.

The yellow ruthenium(II) complexes **1** and **2** were isolated as pure solids from methanol, in reasonable to good yields. The elemental analyses are described in experimental section and they agreed well with the proposed formulations. The molar conductance values measured in methanol at room temperature range from 98 to 104 S cm² mol⁻¹, revealing the 1:1 electrolytic nature of these complexes.²⁷ Complexes are air stable both in the solid state and in DMSO solutions as evaluated by ³¹P{¹H} NMR and UV-Vis experiments for a period of 48 h.

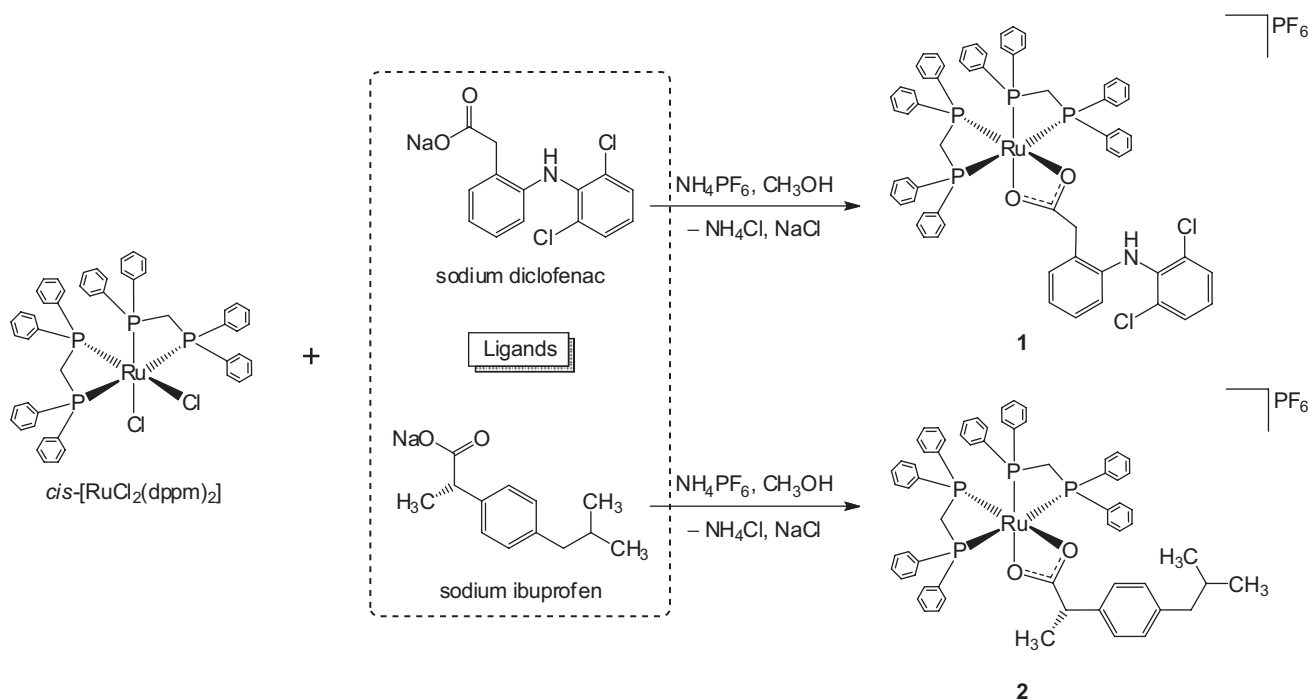
Infrared spectroscopy

The infrared spectra (IR) of complexes **1** and **2** shows the typical asymmetric $\nu_{\text{as}}(\text{COO}^-)$ and symmetric $\nu_{\text{s}}(\text{COO}^-)$ carboxylate stretching frequencies at 1522; 1452 cm⁻¹ (**1**) and 1516; 1461 cm⁻¹ (**2**), respectively, as showed in Figure 2.

The $\Delta\nu$ values of 70 cm⁻¹ for complex **1** and 55 cm⁻¹ for **2** are indicative of a η^2 binding mode of the carboxylate group.²¹ In addition, for complex **1**, characteristic vibrational modes of the diclofenac ligand at 3344 and 1100 cm⁻¹ were observed, corresponding to ν_{NH} and $\nu_{\text{Ph-Cl}}$, respectively. For both compounds the characteristic P-F stretch of the PF₆⁻ counterion was seen at 837 cm⁻¹.²⁸ Most of the vibrational modes observed were characteristic of the dppm ligands occurring practically at same frequencies observed for the precursor *cis*-[RuCl₂(dppm)₂].

X-ray structure analyses

X-ray structure analyses of the complex **2** confirm the IR spectroscopy data. An ORTEP drawing of **2** showing the



Scheme 1. Route for the synthesis of complexes **1** and **2**.

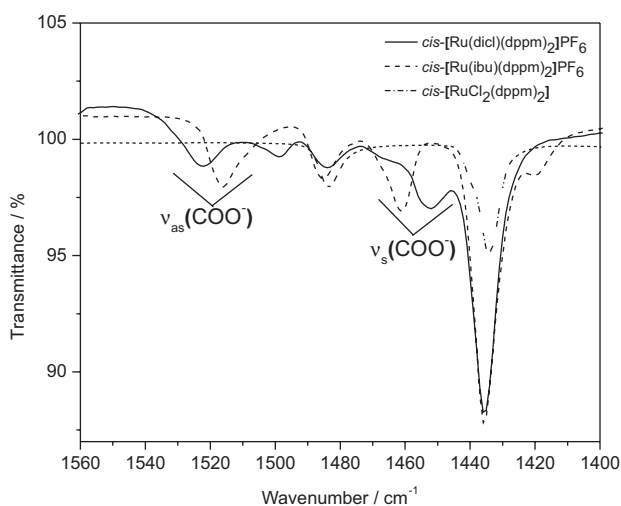


Figure 2. IR spectra of *cis*-[Ru(dicl)(dppm)₂]⁺PF₆⁻ (**1**), *cis*-[Ru(ibu)(dppm)₂]⁺PF₆⁻ (**2**) and *cis*-[RuCl₂(dppm)₂].

atom numbering scheme is depicted in Figure 3. Selected bond lengths and angles are presented in Table 2.

Two disordered positions were refined for the fragment which includes the chiral center C(2) as well as the methyl and hydrogen groups attached to it. The two sites are shown together in Figure 3. The solid lines (labeled A) indicate the bonds between the atoms with higher occupation factor (68.4%), whereas the dashed lines (labeled B) represent the species with the lower occupation (31.6%). Plots showing the major and minor components of the disordered structure observed in **2** separately can be found as supplementary information (Figures S1 and S2). The

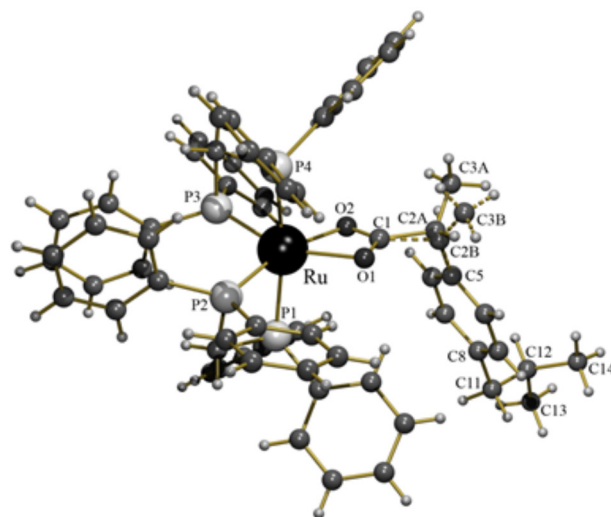


Figure 3. ORTEP view of the cation complex *cis*-[Ru(ibu)(dppm)₂]⁺ (**2**) showing the two disordered forms of ibuprofen ligand. The PF₆⁻ counterion was omitted for clarity.

reason for the disorder can clearly be derived from the orientation of the ligand due to the presence of the chiral center C(2), and consequently, two complex species with the ligand in *R* (major component) and *S* (minor component) configurations could be detected in the solid structure of the compound. Since the ligand used was a racemic mixture of ibuprofen, it is reasonable that both *R* and *S* isomers react with ruthenium(II) precursor. In fact, the ³¹P{¹H} NMR of a powder of complex **2** also shows two set of signals with relative integration 60:40, revealing that these species are also preserved in solution

Table 2. Selected bond distances and angles for complex **2**

Bond	Bond distance / Å	Bond angle	Angle / degree
Ru(1)–O(2)	2.1676(18)	P(3)–Ru(1)–P(2)	92.01(2)
Ru(1)–O(1)	2.217(2)	O(2)–Ru(1)–P(4)	92.17(5)
Ru(1)–P(3)	2.2811(7)	P(2)–Ru(1)–P(1)	70.93(2)
Ru(1)–P(2)	2.2958(7)	P(3)–Ru(1)–P(4)	72.36(2)
Ru(1)–P(4)	2.3204(5)	O(1)–Ru(1)–P(1)	95.52(5)
Ru(1)–P(1)	2.4092(6)	P(4)–Ru(1)–P(1)	170.69(2)
O(1)–C(1)	1.268(4)	O(1)–Ru(1)–P(3)	154.73(6)
O(2)–C(1)	1.251(4)	O(2)–Ru(1)–P(2)	163.77(6)
		O(2)–Ru(1)–O(1)	59.34(9)

(see solution studies). Furthermore, the observation of the two types of isomers in the same crystal is not very common. This can be explained as a case of static disorder where **2** presents the *R* and *S* configurations distributed among different unit cells.²⁹

This compound crystallizes in the orthorhombic system, space group Pna2(1), with the Ru center adopting a distorted octahedral coordination geometry formed by two *cis*-chelating diphosphine ligands and the bidentate (η^2) carboxylate group of the ibuprofen ligand. The distortions are caused by chelation angles of 70.93(2) and 72.36(2)° imposed by the methylene bridge of dpmm ligands and especially by the carboxylate group with an O(1)–Ru–O(2) angle of only 59.34(9)°. This small angle found for the carboxylate group is very similar to that observed for ruthenium(II) complexes containing coordinated acetate and other carboxylates in the bidentate fashion.^{30–32} The Ru–P bond lengths vary from 2.3204(5) to 2.4092(6) Å for mutually *trans* disposed phosphorus atoms and from 2.2811(7) to 2.2958(7) Å for phosphorus atoms *trans* positioned to oxygen atoms from the carboxylate group. These marked differences clearly illustrate the greater *trans*-influence of phosphorus when compared with oxygen.^{31–33} The carboxylate ligand is coordinated with a certain degree of asymmetry as illustrated by the Ru–O distances of 2.1676(18) and 2.217(2) Å. These values are in the range reported for similar compounds.^{30–35} This asymmetry probably is due to some weak interactions of the phenyl group of ibuprofen with adjacent phenyl rings of dpmm. This kind of asymmetry was previously observed for ruthenium(II) ferrocenylcarboxylates.³⁴

³¹P{¹H} Nuclear magnetic resonance (NMR) spectroscopy

The ³¹P{¹H} NMR spectra of complexes **1** and **2** show typical patterns of species containing two *cis* positioned diphosphines and equal ligands completing the octahedral

coordination sphere. For complex **1** a pair of triplets that integrate in 1:1 ratio with chemical shifts at 8.2 and –12.8 ppm was observed. The splitting pattern was consistent with an A₂X₂ ($\Delta\nu / J = 87$) assignment similar to those described for analogous complexes.³⁴ For complex **2** a slightly different behavior was observed. In the more deshielded region two triplets with very close chemical shifts (8.4 and 8.2 ppm) appeared, besides one triplet in the shielded region (–12.3 ppm), as showed in Figure 4.

The integration of the triplets at 8.4 and 8.2 ppm are in the 1:1 ratio with the triplet at –12.3 ppm. This behavior clearly indicates the presence of a mixture of two very similar species and based on the integration of each line of the signals close to 8 ppm it is found a 60:40 ratio between the species. This ratio is in agreement with the two configurations of ibuprofen ligand observed in crystal structure of the complex **2** as previously discussed. The splitting pattern is also consistent with an A₂X₂ assignment with $\Delta\nu / J = 88$ and 87 for each one of the configurations. In addition, since the PF₆[–] counterion was utilized, it was observed the characteristic septet due to the phosphorus-fluorine coupling with chemical shift centered at –144.6 ppm for both complexes.

High-resolution mass spectrometry (HRESI)

Mass spectra of complexes containing ruthenium are typical for their isotopic pattern demonstrated by the presence of ⁹⁶Ru (5.5%), ⁹⁸Ru (1.9%), ⁹⁹Ru (12.7%), ¹⁰⁰Ru (12.6%), ¹⁰¹Ru (17.1%), ¹⁰²Ru (31.6%) and ¹⁰⁴Ru (18.6%) isotopes, with the nuclide abundance in parentheses. Furthermore, complex **1** had a ligand with chlorine (³⁵Cl (75.8%) and ³⁷Cl (24.2%)) which contributes with an additional isotopic pattern (Figure 5). The high-resolution mass spectra of the compounds **1** and **2** were recorded and the obtained data confirm the established pattern (Figures 5a and 5b). In this study, the *m/z* values listed below in the text refer to the peak of the most abundant element corresponding to the ¹⁰²Ru isotope. The HRMS spectra were acquired in the positive mode and the charged complex ions were observed at *m/z* 1164.1520 [M]⁺ (**1**) and 1075.2660 [M]⁺ (**2**), in agreement with calculated values for C₆₄H₅₄Cl₂NO₂P₄Ru, 1164.1520 and C₆₃H₆₁O₂P₄Ru, 1075.2660, respectively. Collision-induced dissociation (CID) experiments (MS/MS) with an increasing collisional energy using N₂ as collision gas under the selected ions at *m/z* 1164.1520 [M]⁺ (**1**) and 1075.2660 [M]⁺ (**2**), showed a fragmentation pathway just for complex **1** even in higher collisional energies. The loss of 295 u was proposed for a neutral elimination of the ligand (diclofenac, acid form) (Figure 5c).

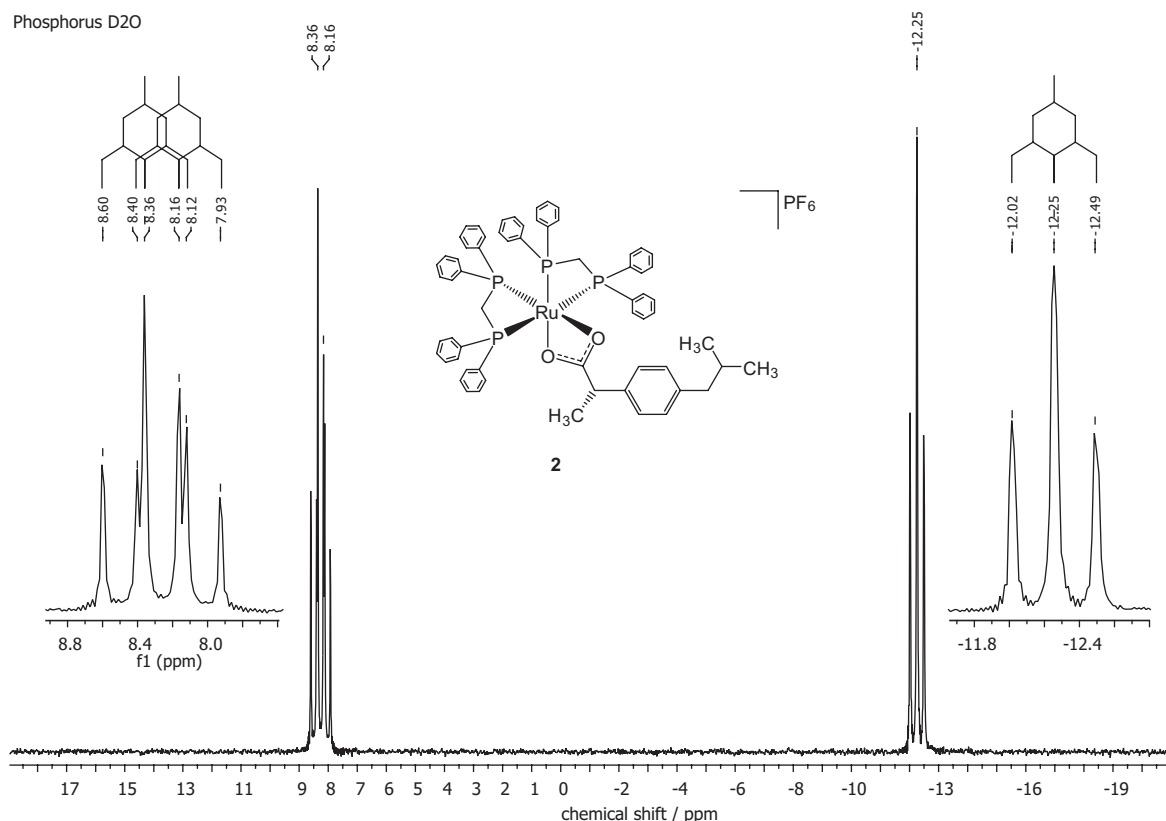


Figure 4. ^{31}P [^1H] NMR spectrum (162.0 MHz, $\text{CH}_2\text{Cl}_2/\text{D}_2\text{O}$) of complex **2**.

Ct-DNA binding studies: UV-Vis spectrophotometrical and viscosity studies

In an attempt to study the nature of the ruthenium complexes interactions with ct-DNA, UV-Vis absorption spectra were obtained by titration of the complexes with increasing concentrations of ct-DNA. The electronic spectra of complexes **1** and **2** showed an intense absorption peak around 264 nm, which could be attributed to an intraligand π - π^* transition of the coordinated groups in the complex, that has been selected to study the spectral changes with ct-DNA addition. Both complexes displayed the same behavior in which absorption decreases with ct-DNA titration, however, this characteristic is attributed only to dilution effects. This was demonstrated by titration of the complexes with buffer solution (not containing ct-DNA) in which the same absorption decrease was observed. All these spectra are showed in supplementary information (Figure S4). These data showed that these complexes do not exhibit covalent or intercalative interactions with ct-DNA.^{36,37} Due to the very weak interaction (hypochromism < 3%) was not possible determine the intrinsic binding constant (K_b) between the ruthenium complexes and ct-DNA.

The possible mode of interaction between complexes and ct-DNA was also evaluated by viscosity experiments. It

is well known that classical intercalators, such as ethidium bromide, lead to an increase in the viscosity of ct-DNA because separation of the base pairs occurs to accommodate the intercalator. A covalent DNA-binding mode may cause its fragmentation, thus decreasing the ct-DNA viscosity.³⁸⁻⁴⁰ However, complexes **1** and **2**, exhibited essentially no effect on the viscosity of ct-DNA as demonstrated in a plot $(\eta/\eta_0)^{1/3}$ versus $[\text{complex}]/[\text{DNA}]$ showed in supplementary information (Figure S5). This result is consistent with existence of electrostatic interactions between ruthenium complexes and ct-DNA.^{25,26} Considering the molecular structure and positive charge of the complexes, electrostatic interactions involving the negatively charged phosphate groups of ct-DNA are expected.

In vitro cytotoxic activity

The human cell lines were exposed to the ruthenium(II) complexes and cisplatin for a period of 24 h, in order to allow them reach DNA or any other biological target. The IC_{50} values, calculated from the dose-survival curves generated by the XTT assays obtained after drug treatment are shown in Table 3.

Complexes **1** and **2** have showed, in general, high cytotoxicity against all the human tumor cell lines assayed

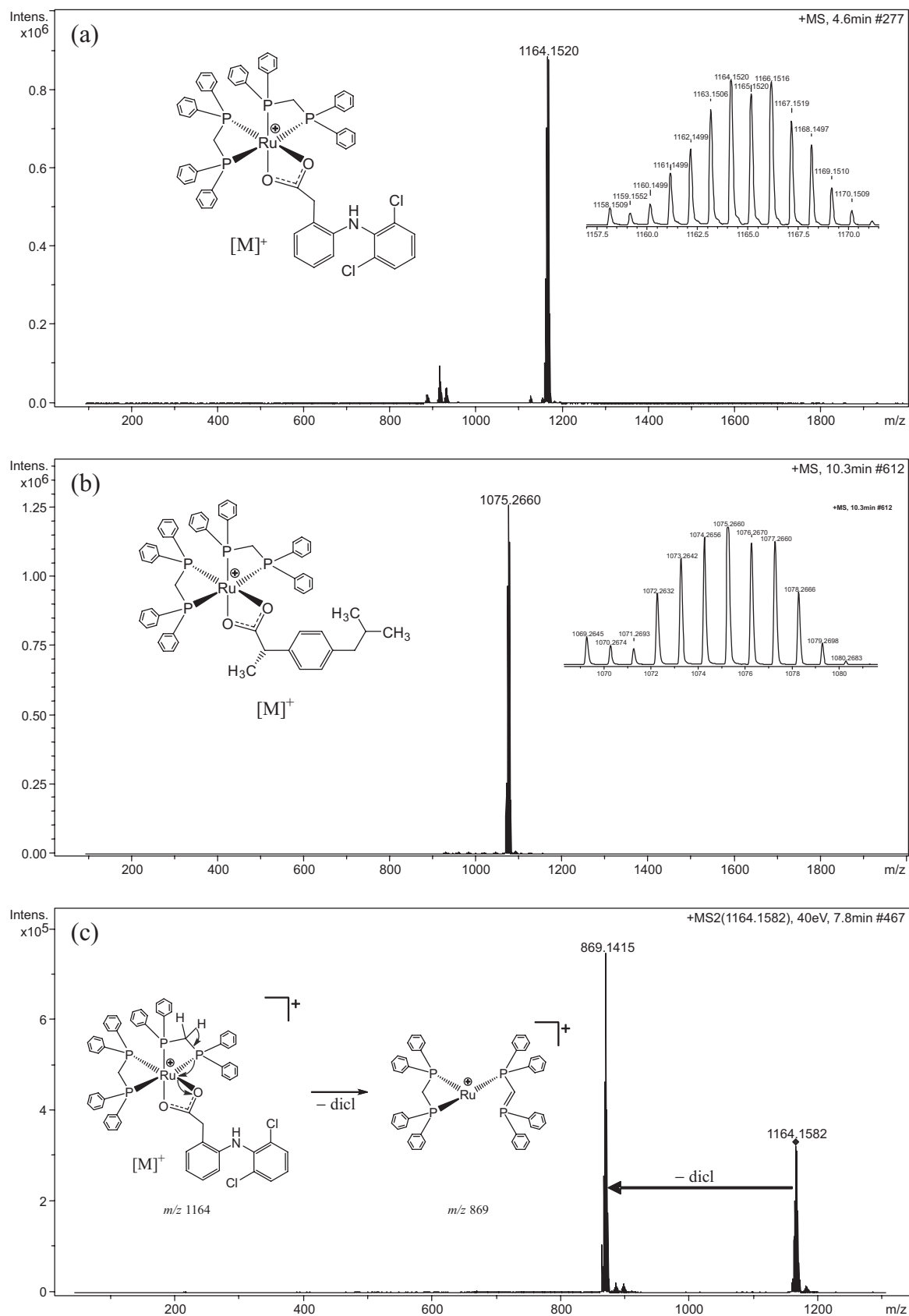


Figure 5. ESI mass spectra of *cis*-[Ru(dicl)(dppm)₂]⁺ (**1**) and *cis*-[Ru(ibu)(dppm)₂]⁺ (**2**). (a) HRESI-MS spectrum of *cis*-[Ru(dicl)(dppm)₂]⁺ *m/z* 1164.1520 [M]⁺ (calcd. for C₆₄H₅₄Cl₂NO₂P₄Ru, 1164.1520); (b) HRESI-MS spectrum of *cis*-[Ru(ibu)(dppm)₂]⁺ *m/z* 1075.2660 [M]⁺ (calcd. for C₆₃H₆₁O₂P₄Ru, 1075.2660) and (c) ESI-MS/MS spectrum of *m/z* 1164.1520.

Table 3. Inhibitory activity of ruthenium(II) complexes and cisplatin against normal and tumor cell lines, expressed as IC₅₀

Compound	Cell line			
	HepG2 ^a	MCF-7 ^b	MO59J ^c	GM07492A ^d
	IC ₅₀ / (μmol L ⁻¹)			
<i>cis</i> -[RuCl ₂ (dppm) ₂]	108 ± 28	191 ± 13	134 ± 10	66 ± 4
1	7.6 ± 0.9	47 ± 6	8 ± 2	2 ± 1
2	5 ± 3	9 ± 3	6.5 ± 0.2	6 ± 2
Cisplatin	6.3 ± 0.7	34 ± 4	22 ± 4	26 ± 3

^aHepG2: hepatocellular carcinoma; ^bMCF-7: breast adenocarcinoma; ^cMO59J: glioblastoma; ^dGM07492A: normal lung fibroblasts.

with IC₅₀ values ranging from 5 to 9 μmol L⁻¹, except for complex **1** in MCF-7 cells that showed a moderate cytotoxicity as presented in Table 3. Complex **2** displayed higher activity than **1** in all the tumor cell lines assayed with similar IC₅₀ values independent of the cell line. This non-selective activity of complex **2** was not observed for complex **1** that was much less cytotoxic in MCF-7 cells. Compared with the reference metallodrug cisplatin, complex **1** displayed approximately the same cytotoxic activity for HepG2 and MCF-7 cells and a three times increased activity for MO59J cells. Complex **2** had similar activity to cisplatin for HepG2 cells and a four times increased activity against MCF-7 and MO59J cells. The selectivity index (SI) (SI = IC₅₀ GM07492A / IC₅₀ human tumor cell line) was smaller than 1 for all the cell lines assayed for complex **1**, while for complex **2** the SI values are very close to 1, both indicating a low selectivity.

Under the same experimental conditions cisplatin also displayed SI values close to 1 for MCF-7 and MO59J tumor cell lines. The precursor complex *cis*-[RuCl₂(dppm)₂] was less active than the complexes **1** and **2** by factors ranging from 4.1 to 21.6. A similar increase in toxicity was observed against the normal cell line GM07492A. These data clearly indicates that the exchange of two chlorido ligands by a bidentate anti-inflammatory molecule makes the *cis*-[Ru(dppm)₂]²⁺ unity complex more cytotoxic, probably due to the different lipophilicity and consequent entrance in the cells. Further experiments concerning the amount of ruthenium complex that gets inside the cells as well as its intracellular targets, beyond DNA, are required to understand details of the observed activity and will be a point of study in a near future.

Conclusions

In this investigation two new ruthenium(II) complexes containing dppm and the anions of anti-inflammatory drugs diclofenac and ibuprofen with formula

[Ru(dicl)(dppm)₂]PF₆ (**1**) and [Ru(ibu)(dppm)₂]PF₆ (**2**) were synthesized and characterized by elemental analysis, X-ray crystallography, spectroscopic and spectrometric methods. The spectroscopic analyses are in agreement with a chelated coordination through the carboxylate group, for the diclofenac and ibuprofen ligands. The crystallographic studies for the ibuprofen derivative revealed two configurations for the ligand in the crystalline structure. Viscosity experiments suggest an electrostatic interaction between ct-DNA and complexes **1** and **2**. The *in vitro* cytotoxicity activity assays of the complexes indicate a high activity against three human tumor cell lines. Indeed one of the complexes was more active than cisplatin against two tumor cells. Interestingly, exchanging chlorido ligands of the *cis*-[RuCl₂(dppm)₂] by diclofenac and ibuprofen resulted in higher cytotoxic activity probably due to the differences in lipophilicity upon complexation influencing the amount of compound that gets inside the cells. Further studies are necessary to verify the biological targets of this class of ruthenium(II) complexes. Although these complexes displayed low selectivity they present potential for the treatment of breast adenocarcinoma and glioblastoma since they present similar SI value to that of cisplatin but a higher activity, so they could be used in lower concentrations.

Supplementary Information

Supplementary information is available free of charge at <http://jbcs.org.br> as PDF file.

Coordinates and other crystallographic data have been deposited with the CCDC, deposition code CCDC 1040297. Copies of the data can be obtained, free of charge, via www.ccdc.cam.ac.uk/conts/retrieving.html or from the Cambridge Crystallographic Data Centre, CCDC, 12 Union Road, Cambridge CB2 1EZ, UK; fax: +44 1223 336033. E-mail: deposit@ccdc.cam.ac.uk.

Acknowledgements

We thank CNPq, CAPES, FAPESP (Grant 2009/54011-8), the Minas Chemical Network and FAPEMIG (Grant APQ-04010-10). The authors are also thankful to the Grupo de Materiais Inorgânicos do Triângulo-GMIT research group supported by FAPEMIG (APQ-00330-14).

References

1. Jamieson, E. R.; Lippard, S. J.; *Chem. Rev.* **1999**, 99, 2467.
2. Wang, D.; Lippard, S. J.; *Nat. Rev. Drug Discov.* **2005**, 4, 307.

3. Dasari, S.; Tchounwou, P. B.; *Eur. J. Pharmacol.* **2014**, *740*, 364.
4. Wheate, N. J.; Walker, S.; Craig, G. E.; Oun, R.; *Dalton Trans.* **2010**, *39*, 8113.
5. Mjos, K. D.; Orvig, C.; *Chem. Rev.* **2014**, *114*, 4540.
6. Barry, N. P. E.; Sadler, P. J.; *Chem. Commun.* **2013**, *49*, 5106.
7. Hartinger, C. G.; Zorbas-Seifried, S.; Jakupec, M. A.; Kynast, B.; Zorbas, H.; Keppler, B. K.; *J. Inorg. Biochem.* **2006**, *100*, 891.
8. Ang, W. H.; Casini, A.; Sava, G.; Dyson, P. J.; *J. Organomet. Chem.* **2011**, *696*, 989.
9. Bergamo, A.; Gaiddon, C.; Schellens, J. H. M.; Beijnen, J. H.; Sava, G.; *J. Inorg. Biochem.* **2012**, *106*, 90.
10. Kostova, I.; *Curr. Med. Chem.* **2006**, *13*, 1085.
11. Bratsos, L.; Jedner, S.; Gianferrara, T.; Alessio, E.; *Chimia* **2007**, *61*, 692.
12. Pillozzi, S.; Gasparoli, L.; Stefanini, M.; Ristori, M.; D'Amico, M.; Alessio, E.; Scaletti, F.; Becchetti, A.; Arcangeli, A.; Messori, L.; *Dalton Trans.* **2014**, *43*, 12150.
13. Trondl, R.; Heffeter, P.; Kowol, C. R.; Jakupec, M. A.; Berger, W.; Keppler, B. K.; *Chem. Sci.* **2014**, *5*, 2925.
14. Hartinger, C. G.; Jakupec, M. A.; Zorbas-Seifried, S.; Groessl, M.; Egger, A.; Berger, W.; Zorbas, H.; Dyson, P. J.; Keppler, B. K.; *Chem. Biodivers.* **2008**, *5*, 2140.
15. Osajca, M.; Kulis, E.; Stochel, G.; Brindell, M.; *New J. Chem.* **2014**, *38*, 3386.
16. Pavan, F. R.; Von Poelhsitz, G.; Nascimento, F. B.; Leite, S. R. A.; Batista, A. A.; Deflon, V. M.; Sato, D. N.; Franzblau, S. G.; Leite, C. Q. F.; *Eur. J. Med. Chem.* **2010**, *45*, 598.
17. Pavan, F. R.; Von Poelhsitz, G.; Cunha, L. V. P.; Barbosa, M. I. F.; Leite, S. R. A.; Batista, A. A.; Cho, S. H.; Franzblau, S. G.; Camargo, M. S.; Resende, F. A.; Varanda, E. A.; Leite, C. Q. F.; *PloS One* **2013**, *8*, e64242.
18. Wang, J.; Hughes, T. P.; Kok, C. H.; Saunders, V. A.; Frede, A.; Groot-Obbink, K.; Osborn, M.; Somogyi, A. A.; D'Andrea, R. J.; White, D. L.; *Br. J. Cancer* **2012**, *106*, 1772.
19. Moser, P.; Sallmann, A.; Wiesenberger, I.; *J. Med. Chem.* **1990**, *33*, 2358.
20. Dahl, J. B.; Kehlet, H.; *Br. J. Anaesth.* **1991**, *66*, 703.
21. Sullivan, B. P.; Meyer, T. J.; *Inorg. Chem.* **1982**, *21*, 1037.
22. Sheldrick, G. M.; *SHELXS-97; Program for Crystal Structure Resolution*; University of Göttingen, Germany, 1997.
23. Sheldrick, G. M.; *SHELXL-97; Program for Crystal Structures Analysis*; University of Göttingen, Germany, 1997.
24. Cohen, G.; Eisenberg, H.; *Biopolymers* **1969**, *8*, 45.
25. Satyanarayana, S.; Dabrowiak, J. C.; Chaires, J. B.; *Biochemistry* **1993**, *32*, 2573.
26. Satyanarayana, S.; Dabrowiak, J. C.; Chaires, J. B.; *Biochemistry* **1992**, *31*, 9319.
27. Geary, W. J.; *Coord. Chem. Rev.* **1971**, *7*, 81.
28. Nakamoto, K.; *Infrared and Raman Spectra of Inorganic and Coordination Compounds*, 5th ed.; Wiley-Interscience: New York, 1997.
29. Muller, P.; Herbst-Irner, R.; Spek, A. L.; Schneider, T. R.; Sawaya, M. R.; *Crystal Structure Refinement: a Crystallographer's Guide to SHELXL*, Oxford University Press: New York, 2006.
30. Jia, G. C.; Rheingold, A. L.; Haggerty, B. S.; Meek, D. W.; *Inorg. Chem.* **1992**, *31*, 900.
31. Murray, A. H.; Yue, Z.; Wallbank, A. I.; Cameron, T. S.; Vadavi, R.; MacLean, B. J.; Aquino, M. A. S.; *Polyhedron* **2008**, *27*, 1270.
32. Lucas, N. T.; Powell, C. E.; Humphrey, M. G.; *Acta Crystallogr. C* **2000**, *56*, 392.
33. Coe, B. J.; Glenwright, S. J.; *Coord. Chem. Rev.* **2000**, *203*, 5.
34. Wyman, I. W.; Burchell, T. J.; Robertson, K. N.; Cameron, T. S.; Aquino, M. A. S. *Organometallics* **2004**, *23*, 5353.
35. Sanchez-Delgado, R. A.; Thewalt, U.; Valencia, N.; Andriollo, A.; Marquezsilva, R. L.; Puga, J.; Schollhorn, H.; Klein, H. P.; *Inorg. Chem.* **1986**, *25*, 1097.
36. Zhang, Q. L.; Liu, J. G.; Chao, H.; Xue, G. Q.; Ji, L. N.; *J. Inorg. Biochem.* **2001**, *83*, 49.
37. Kalaivani, P.; Prabhakaran, R.; Dallemer, F.; Vaishnavi, E.; Poornima, P.; Vijaya Padma, V.; Renganathan, R.; Natarajan, K.; *J. Organomet. Chem.* **2014**, *762*, 67.
38. Sellamuthu, A.; Ravishankaran, R.; Karande, A. A.; Kandaswamy, M.; *Dalton Trans.* **2012**, *41*, 12970.
39. Zivec, P.; Perdih, F.; Turel, I.; Giester, G.; Psomas, G.; *J. Inorg. Biochem.* **2012**, *117*, 35.
40. Navarro, M.; Castro, W.; Higuera-Padilla, A. R.; Sierraalta, A.; Abad, M. J.; Taylor, P.; Sanchez-Delgado, R. A.; *J. Inorg. Biochem.* **2011**, *105*, 1684.

Submitted: April 23, 2015

Published online: June 30, 2015

FAPESP has sponsored the publication of this article.